CFD TRANSIENT SIMULATION OF FOULING IN AN EGR COOLER IN A DIESEL EXHAUST ENVIRONMENT

M.C. Paz, E. Suárez, M. Concheiro, J. Porteiro

Escuela de Ingeniería Industrial, University of Vigo, Lagoas Marcosende 9, CP-36310 Vigo (Spain) cpaz@uvigo.es

ABSTRACT

The most common technology to reduce the amount of NOx emitted in modern diesel engines is the exhaust gas recirculation (EGR) system. This method use a gas-coolant heat exchanger usually, the EGR cooler, which suffer the fouling effects. The application of a previous 3D transient fouling model based on the soot deposition-removal balance to a real EGR cooler is presented. The CFD implementation of the model is done in ANSYS-Fluent. The results are compared to experimental data of the cooler working in an exhaust environment. The results obtained confirm that performance degradation over time of the complete cooler can be predicted in good agreement with a reasonable computational cost. Also the importance of each mechanism is discussed.

INTRODUCTION

The pollutant emission limits from internal combustion engines have led manufacturers to develop a range of different devices and technologies to satisfy the current standards.

One of the most widely used, reasonably priced and consolidated techniques to reduce NOx emissions is the exhaust gas recirculation (EGR) system. EGR systems recirculate a fraction of the exhaust gases, under certain engine operating conditions, to the intake manifold, where gases are mixed with fresh air, and thus, the subsequent combustion process begins with a lower oxygen concentration. The mixture reduces the peak flame temperature and consequently, decreases NOx formation.

If the gas is directly recycled, the system is called a hot EGR; although, the majority of recirculation systems, even in gasoline engines, include a gas-coolant heat exchanger in the operation, i.e., the EGR-cooler. Most diesel engines are typically turbocharged, and thus, depending on the recirculation location, they are classified as either two system types: high- or low-pressure-loop EGRs (Zheng, 2004). Several aspects are critical in the design of these heat exchangers, same of which depend on the type:

- Pressure drop of the cooler must be seriously limited, particularly in low-pressure-loop EGR systems.

- The compactness of the system is always a goal in automotive engineering, which implies a high thermal efficiency requirement.
- Coolant flow rate limitations, coupled with the previous item, imply boiling prevention or control of another important design parameter.
- Difficult and variable working conditions make thermal fatigue cycle analysis a common requisite.
- Pressure pulses present in exhaust gases promote fluctuating forces, which may cause unexpected structural failures.
- The depositions of residue on heat transfer walls, mainly on the gas side, negatively affect thermal efficiency (Teng and Regner, 2009).

Several papers (Epstein, 1981; Müller-Steinhagen and Middis, 1989; Thonon et al., 1999; Stolz et al., 2001) agree that fouling follows an asymptotic evolution. This process is characterised by a rapid growth of the deposited layer in the first stages and a progressively slower growth until stable asymptotic conditions are reached. The entire process generally occurs in a matter of hours (Grillot and Icart, 1997; Abd-Elhady et al., 2011); therefore, the heat exchanger works almost its entire lifetime under fouled conditions. The deposition of fouling material on heat transfer walls causes an increase in thermal resistance due to the low conductivity of the residue, and therefore, the global thermal efficiency is reduced by fouling (Marner, 1990; Lepperhoff and Houben, 1993; Bott and Melo, 1997; Park et al., 2010).

The thickness of the deposited layer, soot and hydrocarbons (Hoard et al., 2008) primarily decreases the free-flow section, changes the velocity field, boundary layer separation and reattachment locations with respect to clean conditions and changes the turbulence field. These changes cause an increase in the gas pressure drop through the cooler (Hesselgreaves, 1992).

The modelling of fouling process in EGR cooler systems has been previously studied. Some of the works are 1D models applied to a 1D approximation of the geometry and usually with no erosion or re-entrainment mechanisms included, (Abarham et al., 2009b, Abarham et al., 2013). Other studies employ a Lagrangian framework

for the particle transport on a simplified channel of the heat exchanger, (Nagendra et al., 2011), or a complete steady 3D model applied to a single tube (Stauch et al., 2011). Apart from the latest work of Abarham (Abarham et al. 2013), no fouling depth prediction is made by none of the above mentioned references.

In general, most of the methods and models already published are based on bulk conditions or non-local parameters. Thus, their applicability is limited to simple geometries (1D, axi-symmetric, single channel, etc) where, thanks to the homogeneity of the flow, those parameters can be undoubtedly defined. In industrial geometries, and especially in automotive applications, the aforementioned limitation is particularly strong due to entrance effects, cross-section changes, thermal gradient variation along the heat exchanger, non-developed thermal and viscous boundary layer conditions, etc. which may have a strong impact on fouling layer evolution. Thus, the implementation of a CFD fouling algorithm requires a cell-based formulation, therefore the flow magnitudes have to be obtained at each cell.

In a previous work, Paz et al. (Paz et al., 2013) developed a computational fouling model, which was validated through its application to a reference geometry exposed to diesel exhaust gases. The model is based on the deposition-removal balance and was applied to the exterior of round cooled tubes positioned traversed to the gas flow. This model locally reproduced the local fouling thickness with good agreement under the constant thermal and flow conditions being imposed in the tests.

The objective of the present study is to apply this fouling model to a complete EGR cooler. Global and local results are analysed, and the importance of the existing mechanisms will be discussed. Fouling layer thickness profiles are analysed, and the cooler performance evolution over time are compared with experimental results.

GEOMETRY

The geometry used is a shell-and-tube configuration. The exhaust gases flow inside the tubes, and the coolant flows between the shell and the tubes. The dimensions correspond to typical sizes of compact heat exchangers used in passenger cars. Details concerning tube length, diameters and flow direction are presented in Figure 1.

A tube bundle of nineteen round smooth tubes of 8 mm diameter has been taken into account. Although smooth tubes are less widely used than enhanced surfaces nowadays, this less complex geometry was considered for simplification purposes. The primary conclusions are valid since both the main flow characteristics and the fouling thickness evolution predicted by the model are representative of the current technology.
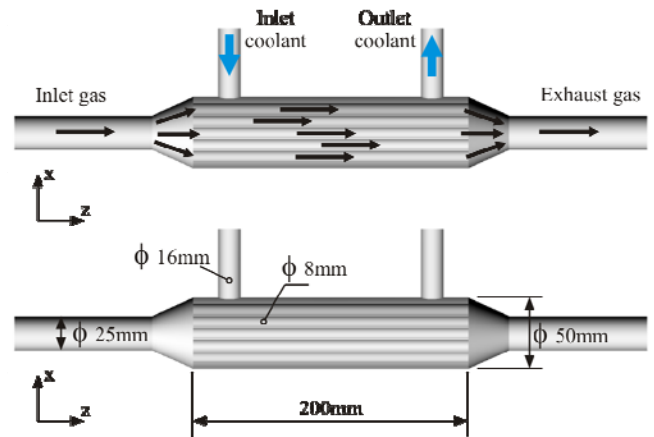
Fig. 1 Geometry of the EGR-cooler.

All parts of this EGR cooler were considered as stainless steel. The thickness of the tubes are 0.25 mm, the diameters of the inlet and outlet header are 1.5 mm, and the diameters of the spigots, external tubes and conical connections are 1 mm.

A detailed view of the header with the tubes numbered from left to right and top to bottom is presented in Figure 2.
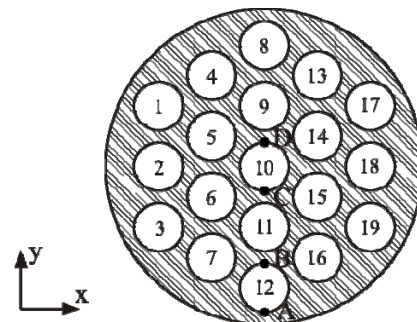
Fig. 2 Detailed schematic of inlet header and tubes.

NUMERICAL MODEL

Mesh

The geometry and mesh of the simulated cooler were generated using GAMBITtm and T-GRID, the preprocessing modules of Fluent.

The mesh convergence criterion was evaluated by simulating a characteristic region of the system, one tube, with different mesh sizes. The results of this study showed that the surface mesh size is not the primary restrictive parameter, and convergence was achieved with mesh size values larger than 3 mm. The final surface mesh created was 1 mm in size.

In accordance with the numerical implementation of the fouling model, a boundary layer larger than usual is necessary to allow the growth of the surface elements representing the fouling layer. Hence, the boundary layer was divided into two regions: a region adjacent to the wall, with 30 uniform prismatic layers, with a size adjusted to attain a y^+ of approximately 1; and the region distant from the wall, 20 prismatic cells with a linear volumetric growth of 20% was used to achieve a smooth transition. The inner region was meshed with unstructured tetrahedral cells. The

final mesh was comprised of more than $12 \cdot 10^6$ cells, whose main quality parameters are summarised in Table 1.

Table 1. Main quality parameter values of the mesh.

	Skewness	Size change	Aspect ratio	Squish
Max.	0.76	6.1	26	0.81
Avg.	0.15	1.07	3.06	0.12

Fouling Model

The fouling model was described in the previous paper by Paz et al. (Paz et al., 2013). Hence, we will not describe an exhaustive extension of the model formulation as details regarding the model have already been presented in the aforementioned work.

The implementation and coupling of the fouling model (Suárez et al., 2010) was developed with the commercial code ANSYS Fluent 6.3.26. The model implementation was adapted and integrated into ANSYS 14.5. The model is based on soot particle deposition neglecting condensation and is a semi-empirical and phenomenological model that takes local effects into account. The sticking probability S_d was taken as one, and the strength bond factor ξ was adjusted experimentally.

The model is based on the deposition and removal dimensionless velocities. The deposition velocity is the sum of two contributions: mass diffusion u^+_{di} and thermophoresis u^+_{th}, which is generally the most important deposition force when thermal gradients are present (Eisner and Rosner, 1985; Messerer et al., 2003;) with typical soot particle sizes between 10^{-8} to 10^{-5} m (Kittelson, 1998). The mechanisms leading to re-entrainment of deposited particles are not totally understood and there is no confirmed theory. The normal description of the physical process relates aerodynamic drag, rotation and lift forces with the local velocity profile incident on the particle. Different researchers analysed removal and its limits, some of them quantifying the process through the average velocity while others rely on a shear stress at the wall (Abd-Elhady et al., 2013; Sluder, 2013; Abd-Elhady et al., 2011; Abd-Elhady et al., 2004). In this work, the removal dimensionless velocity is considered proportional to the layer thickness and the wall shear stress, (Freeman et al., 1990; Kim and Webb, 1991; Bott, 1995).

A summary of the main model equations implemented in the code is presented in Figure 3. Once the velocities are computed for each cell, the external time evolution of this unsteady process allows for the calculation of the net fouling thickness deposited, x_f, at the end of the time step. The net thickness is then virtually accumulated in the cells adjacent to the walls, until the height of a cell is exceeded; at this moment, the fluid cell is changed to a solid cell with its corresponding physical properties. Note that this process is reversible; a fouled cell can be removed, i.e., become a fluid cell again if there are changes in the flow conditions and the newly computed x_f is smaller than the cell size. The deposit properties used were an effective density of 36.5 kg/m^3 and a thermal conductivity of 0.07 W/m·K, which have been obtained by experimental adjustment in a previous work (Paz et al., 2009). In this work fouling factor evolution curves were fitted to asymptotic profile and deposit mass were weighted, under 30 to 60 kg/h exhaust gases flow at 400ºC.

The proposed local methodology allows for time reconstruction of fouling, which systematically affects the thermal efficiency and flow field, increases the thermal resistance of the wall with the thermal insulating layer and also modifies the geometry of the domain.

Boundary conditions/model set-up

All the walls have a no-slip momentum condition. The thermal conditions were coupled for tube walls and headers, with adiabatic conditions for all the other walls insulated in the experimental test. The exhaust gas and coolant inlets were simulated as mass flow inlets, and both exits were considered as outflows. The following are the imposed flow conditions simulated: 60 kg/h of exhaust gas at 400ºC, and 1000 L/h of coolant at 90ºC. The exhaust gas was simulated as ideal gas with a particulate concentration $C_b = 10^{-3}$ kg/Nm^3 and with a sticking probability of $S_d=1$. These values correspond to typical experimental values and were also used in the experimental workbench. The corresponding local maximum gas velocity in its different sections is between 35 and 90 m/s which is the normal range of operation of this kind of equipment.

Water was employed as coolant with Fluent's default properties. A low Mach number was verified for the entire gas domain, and thus, the gas was treated as an incompressible, ideal gas. The gas viscosity was modelled following the three-coefficient Sutherland method. k–ε realizable turbulent model was used, with the near wall treatment "enhanced wall treatment" (ANSYS, 2008) imposed by the size of the cells required at the wall to precisely account for the evolution of the fouling layer. A pressure-based solver was used with the SIMPLE pressure-velocity coupling scheme. Momentum and turbulence equations were solved with the high-order QUICK scheme.

$$C_S = 1.17 \quad C_t = 2.18 \quad C_m = 1.14$$

$$\underbrace{\lambda_g \; u_\tau \; \lambda_p \; \nabla T \; v \; T}$$

$$u_{th}^+ = -\frac{2C_S}{1+3C_m \cdot Kn} \cdot \frac{\frac{\lambda_g}{\lambda_p} + C_t \cdot Kn}{1+2 \cdot \frac{\lambda_g}{\lambda_p} + 2C_t \cdot Kn} \cdot \frac{v \cdot C_C \cdot \nabla T}{u_\tau \cdot T}$$

$$C_c = 1 + \frac{2l}{d_p}\left(1.257 + 0.4 \cdot e^{1.1\,d_p/2l}\right)$$

$$\left.\begin{array}{c} v \; M \\ R \; T \end{array}\right\}$$

$$l = 2\,v\sqrt{\frac{\pi M}{RT}} \quad Kn = \frac{2 \cdot l}{d_p}$$

$$\left.\begin{array}{c} u_\tau \; \rho \\ \mu \; T \\ \rho_p \; d_p \end{array}\right\} \quad \tau_p^+ = \frac{\rho_p \cdot d_p^2 \cdot \rho \cdot u_\tau^2}{18 \cdot \mu^2}$$

$$u_{di}^+ = 0.057 \cdot Sc^{-2/3} + 4.5 \cdot 10^{-4} \tau_p^{+2}$$

$$\left.\begin{array}{c} \mu \; K_B \\ d_p \; T \end{array}\right\}$$

$$D = \frac{K_B \cdot T}{3 \cdot \pi \cdot \mu \cdot d_p} \quad Sc = \frac{\mu}{\rho \cdot D}$$

$$\left.\begin{array}{c} \Delta t \; C_b \\ \rho_f \; S_d \end{array}\right\} \quad x_d = \frac{S_d \cdot (u_{di} + u_{th}) \cdot C_b}{\rho_f} \cdot \Delta t$$

$$\left.\begin{array}{c} a_1, \, a_2, \, a_3, \, a_4 \\ x_f \; \tau_w \; \Delta t \end{array}\right\}$$

$$\xi = a_1 - \left(\frac{a_1 - a_2}{1 + e^{a_3(\tau_w - a_4)}}\right) \quad x_r = \frac{\tau_w \cdot x_f}{\xi} \cdot \Delta t$$

$$x_f = x_d - x_r$$
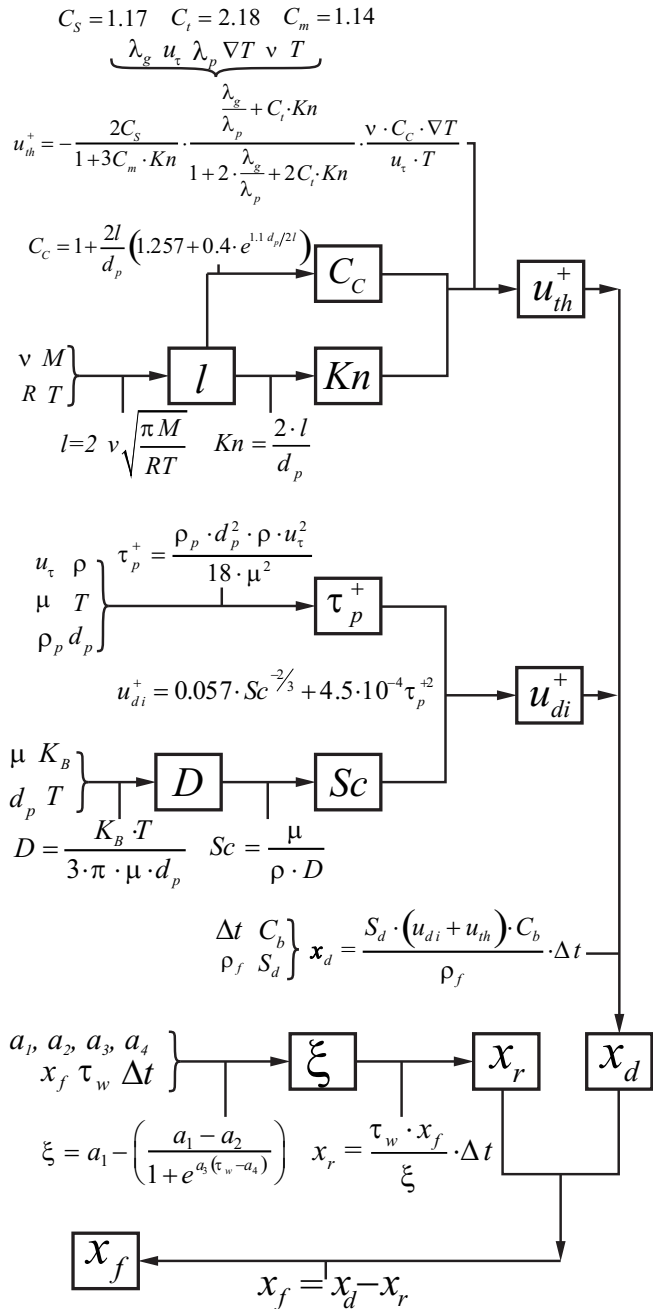
Fig. 3 Summary of fouling model equations (Paz et al., 2013).

RESULTS AND DISCUSSION

The results will be presented in two parts, first the global results, corresponding to the complete cooler performance, and second, the results from a local point of view.

Cooler performance evolution:

Although comparing CFD fouling model results with experimental data was not the primary objective of this research, the EGR cooler was tested experimentally. The experiment was performed under the same boundary conditions that were simulated. The test bench was the same that was used on the previous fouling model validation (Paz

et al., 2009), and the end of the test was established once the experimental fouling factor had reached asymptotic behaviour.

During the test, the thermal efficiency time evolution was obtained, which is presented in Figure 4, and compared with that predicted by the fouling model.
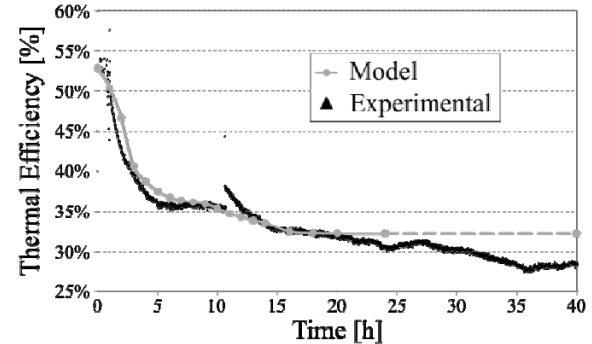
Fig. 4 Thermal efficiency evolution.

The evolution profile agrees exceptionally well in terms of the clean efficiency, which is approximately 55% after 20 hours of simulation. Afterwards, the fouling model reached its asymptotic conditions, whereas the experimental data exhibited a continual decrease of approximately 4% more. Despite this difference, the prediction of the thermal efficiency evolution is considered satisfactory.

Before and after the test, the cooler was weighed (after removing moisture in a drying oven), where the difference was 2.77 grams, which is considered the deposited fouling mass. In the cooler simulation, it is possible to analyse the evolution of the deposited mass, as shown in Figure 5.
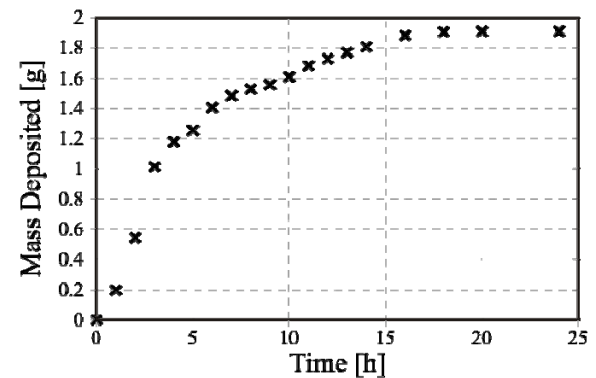
Fig. 5 CFD prediction of deposited mass.

The differences can be attributed to errors in the density used to create the fouling layer; however, the mass estimation is of the same order of magnitude and is therefore considered acceptable.

Due to technical problems in the acquisition of pressure drop during the fouling tests no experimental results are available. The pressure drop increase of the numerical prediction goes from 14.9 mbar for clean conditions to 19.0 mbar once asymptotic conditions were reached; these results agree with similar tests (Abarham et al., 2009). The obtained results confirm that the global cooler performance can be predicted in acceptable agreement with the experimental data obtained from the real engine tests.

Local results:

The flow distribution in the tubes is non-uniform, as shown from the mass flow distribution of each tube in Figure 6.
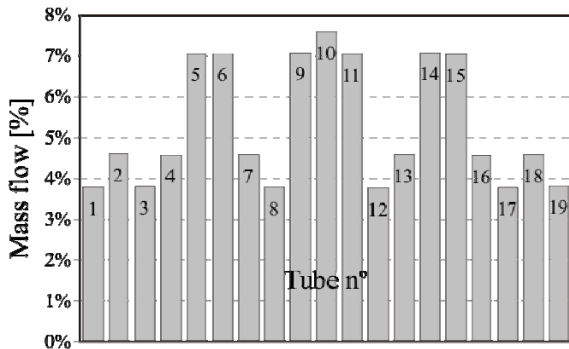
Fig. 6 Distribution of mass flow per tube.

Due to the geometry of the cooler, central tubes have a greater mass flow than that of external tubes. This flow distribution produces non-uniform wall shear stress patterns, which explains the large fouling differences between tubes. Tubes with a greater flow rate and therefore, a higher velocity and higher wall shear stress, have a greater removal velocity, and as a result, a smaller deposited thickness. In Figure 7, the average fouling thickness per tube is compared with the corresponding tube mass flow, which exhibits a clear decreasing tendency.
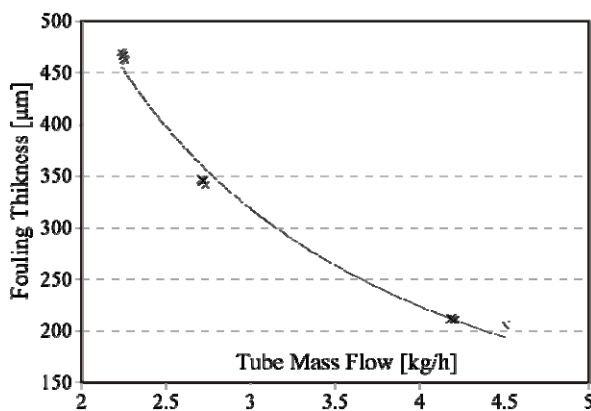
Fig. 7 Average fouling thickness per tube vs. tube mass flow.

These results agree with previous experimental evidence that the greatest part of the residue was deposited in areas where shear forces are small (Bouris, 2005; Paz et al., 2012). The experimental results were verified visually, and the minimum fouling thicknesses correspond with the areas simulated where the wall shear stress was at its maximum.

Furthermore, the results of the average and maximum fouling thickness on different walls of the cooler were compared and are presented in Table 2. A remarkable result is the difference between fouling deposited on the headers, since the average thickness is nearly three times larger on the outer header than on the inlet. This difference cannot be attributable only to thermophoresis degradation in the inlet

region due to the layer of soot deposited. Also, the removal velocity, hence, the fluid friction velocity u_τ, should play an important role in these. Friction is greater in the particle-impact region of the inlet header than in the shadow region of the outer header, where deposition conditions are not so heavily counteracted by friction.

Table 2. Fouling thicknesses on cooler walls.

	Avg. Thickness [mm]	Max. Thickness [mm]
Tubes	0.33	0.86
Inlet header	0.21	0.84
Outlet header	0.59	0.93
Conical surf in	0.38	0.88
Conical surf out	0.45	0.88

On the other elements, the differences are less significant, all of which are consistent with the notion that removal makes the difference. The conical surfaces show the same behaviour as the headers, but with less difference.

(a)

(b)
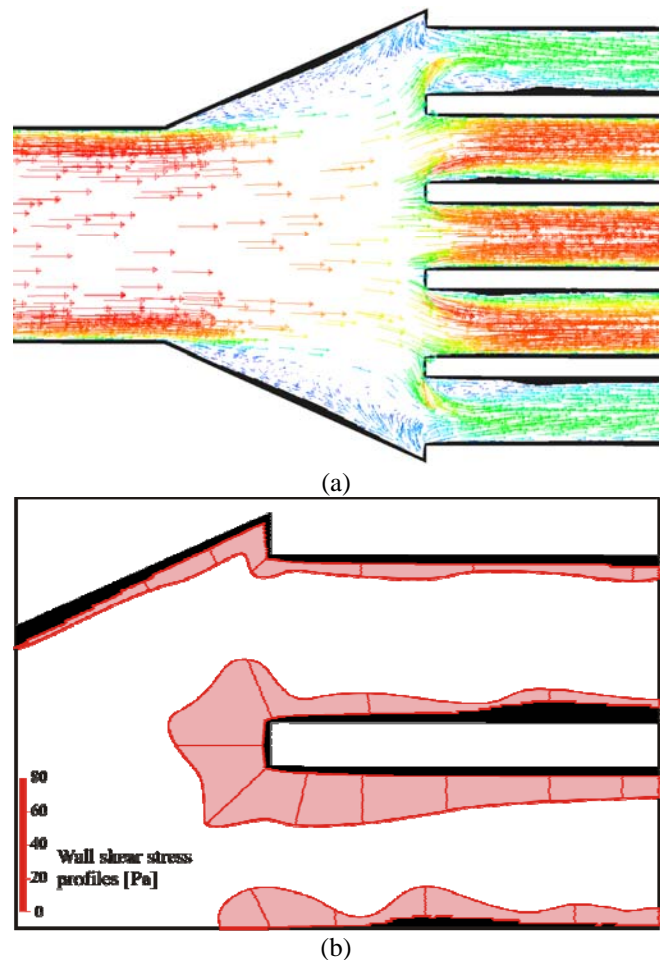
Fig. 8 (a) Velocity pattern and (b) Wall shear stress profile at the entrance of the tubes.

To have a more visual representation of the local effects that occur in the cooler, velocity vectors and wall shear stress profiles of the inlet region are shown in Figure 8. These results correspond to the asymptotic fouling

condition. The figure highlights the heterogeneity of the fouling layer thickness and allows the visualisation of eddies that through erosion, helps clean the header and tip of the tubes.

The three-dimensional vortices and swirls generated in the inlet and outlet region of the tubes create different fouling behaviours around each tube axis. In Figures 9 and 10, the predicted fouling thickness along the tubes length is presented. Profiles A, B, C, and D, correspond with the nomenclature shown in Figure 2. Flow direction goes from left to right, and thus, the thermal gradient decreases from left to right.

The thickness trend of profiles C and D (Figure 9) correspond to central tube 10, which is expected for all the tubes. Moving along the tube, the deposit thickness decreases in the same way as the thermal gradients along the heat exchanger also decrease. As shown, there are no significant differences between the two profiles. These profiles agree with previous studies, highlighting an important dependence between the final deposited thickness and the temperature gradient. Additionally, the aforementioned thermophoresis effect is particularly intense in the typical range of diesel exhaust gases, submicron soot particles and compact heat exchanger environments.
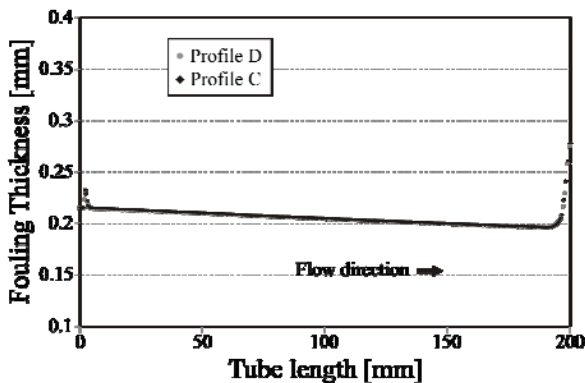
Fig. 9 Fouling thickness profile throughout tube 10.

However, the obtained tendency of fouling is not as clear as we previously expected regarding profiles A and B, which correspond to tube number 12 (Figure 10). These thickness layers show a very different behaviour and are not in harmony with each other, as was the case for tube 10. These differences can be explained because both profiles are affected by different flow conditions, i.e., the flow irregularity shown in Figure 8. Advancing along the tube length, the profiles get closer. In the second half of the tube, they are almost coincident until reaching the final part of the tube, where both layers are again affected by the instabilities associated with turbulence and eddies formed in the discharge of the tube.
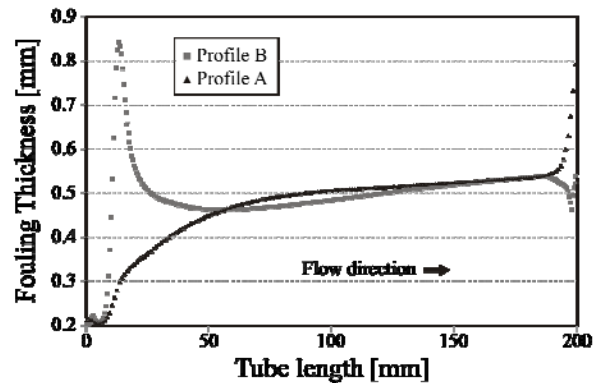
Fig. 10 Fouling thickness profile throughout tube12.

The different local fouling thicknesses obtained in this area of the simulation indicate that in the deposition-removal balance, which is what the model is based on, under the conditions tested and with the fouling model implemented, the relative weight of the erosive effects is greater than that of thermophoresis.

To confirm this result, we plan in the future to try to measure the fouling thickness inside the tubes for further confirmation of the local model predictions.

CONCLUSIONS

In this work a 3D transient fouling model was applied to a complete EGR-cooler CFD simulation, focused on the applicability of the methodology to predict the loss of performance of the real heat exchanger under normal diesel operating conditions.

The simulation was carried out at a reasonable computational cost and without any special requirements other than refinement and using a controlled mesh structure near the wall. The transformation methodology of cells from fluid to solid, which permitted us to obtain the variable fouling thicknesses, was successfully implemented in a complex 3D geometry.

The results of the model were compared with the performance of the same cooler being tested in a diesel engine test-bench. The predicted global results of the cooler performance evolution over time are in good agreement with the experimental data.

Additionally, the particle and fluid local phenomena due to geometrical details such as expansion and contractions greatly affects the fouling deposit obtained.

NOMENCLATURE

a_i Experimental fit constants, dimensionless
C_b Bulk particle concentration, kg m^{-3}
C_C Stokes-Cunningham slip correction factor, dimensionless
$C_{t,m,s}$ Thermophoresis constants, dimensionless
D Mass diffusivity, πr^2, m^2
Kn Knudsen number, dimensionless
l Mean free path, m
Sc Schmidt number, dimensionless

S_d Sticking probability, dimensionless
t Time, s
T Temperature, K
u^+_{di} Isothermal deposition velocity, dimensionless
u^+_{th} Thermophoretic deposition velocity, dimensionless
u_τ Fluid friction velocity, m s^{-1}
x_f Fouling thickness, m
λ Conductivity, W m^{-1} K^{-1}
ρ Density, kg m^{-3}
τ_w Wall shear stress, Pa
υ Kinematic viscosity, m^2 s^{-1}
ξ Strength bond factor, kg m^{-1} s^{-1}

Subscript
d deposition
f fouled
g gas
p particulate
r removal

Superscript
$+$ Dimensionless
$*$ Asymptotic

REFERENCES

M. Abarham, J. Hoard, D. Assanis, D. Styles, E. W. Curtis, N. Ramesh, C. S. Sluder, and J. M. E. Storey, 2009, Modeling of thermophoretic soot deposition and hydrocarbon condensation in EGR coolers. Society of Automotive Engineering, no. 01-1939.

M. Abarham, J. Hoard, D. Assanis, D. Styles, E. Curtis, N. Ramesh, C. S. Sluder and J. M. E. Storey, 2009, Numerical Modeling and Experimental Investigations of EGR Cooler Fouling in a Diesel Engine. Society of Automotive Engineers, no. 2009-01-1506

M. Abarham, P. Zamankhan, J. W. Hoard, D. Styles, C. S. Sluder, J. M. E. Storey, M. J. Lance and D. Assanis, 2013, CFD analysis of particle transport in axi-symmetric tube flows under the influence of thermophoretic force. Heat and Mass Transfer, Vol. 61, pp. 94-105.

M. Abd-Elhady, and M. Malayeri, 2013, Asymptotic characteristics of particulate deposit formation in exhaust gas recirculation (EGR) coolers. Applied Thermal Engineering, Vol. 60, pp. 96-104.

M. S. Abd-Elhady, M. R. Malayeri, and H. M. Müller-Steinhagen, 2011, Fouling Problems in Exhaust Gas Recirculation Coolers in the Automotive Industry. Heat Transfer Engineering, Vol. 32, pp. 248-257.

M. S. Abd-Elhady, C. C. M. Rindt, J. G. Wijers, A. A. van Steenhoven, E. A. Bramer, and T. H. van der Meer, 2004, Minimum gas speed in heat exchangers to avoid particulate fouling. International Journal of Heat and Mass Transfer, Vol. 47, pp. 3943-3955.

M. Abd-Elhady, T. Zornek, M. Malayeri, S. Balestrino, P. Szymkowicz, and H. Müller-Steinhagen, 2011, Influence of gas velocity on particulate fouling of exhaust gas recirculation coolers.

International Journal of Heat and Mass Transfer, Vol. 54, pp. 838-846.

ANSYS, 2008, Fluent User Guide, ANSYS Inc., Lebanon, NH.

D. Bouris, E. Konstantinidis, S. Balabani, D. Castiglia, and G. Bergeles, 2005, Design of a novel, intensified heat exchanger for reduced fouling rates. International Journal of Heat and Mass Transfer, Vol. 48, pp. 3817-3832.

T. R. Bott, 1995, Fouling of Heat Exchangers. Elsevier Ltd, pp. 522.

T. R. Bott, and L. F. Melo, 1997, Fouling of heat exchangers, Experimental Thermal and Fluid Science, Vol. 14, pp. 315.

A. D. Eisner, and D.E. Rosner, 1985, Experimental studies of soot particle thermophoresis in nonisothermal combustion gases using thermocouple response techniques, Combustion and Flame, Vol. 61-2, pp. 153-166.

N. Epstein, 1981, Fouling: Technical aspects. Fouling of heat transfer equipment, pp. 31-53.

W. B. Freeman, J. Middis, and H.M. Müller-Steinhagen, 1990, Influence of augmented surfaces and of surface finish on particulate fouling in double pipe heat exchangers, Chemical Engineering and Processing, Vol. 27, pp. 1-11.

J. M. Grillot, and G. Icart, 1997, Fouling of a cylindrical probe and a finned tube bundle in a diesel exhaust environment. Experimental Thermal and Fluid Science, Vol. 14, pp. 442-454.

J. E. Hesselgreaves (1992). The effect of system parameters on the fouling performance of heat exchangers, Proceedings of the 3rd UK National Conference on Heat Transfer and 1st European Conference on Thermal Sciences.

J. Hoard, M. Abarham, D. Styles, J. M. Giuliano, C. S. Sluder, and J. M. E. Storey, 2008, Diesel EGR Cooler Fouling. Society of Automotive Engineers, no. 01-2475.

N. H. Kim, and R. L. Webb, 1991, Particulate fouling of water in tubes having a two-dimensional roughness geometry. International Journal of Heat and Mass Transfer, Vol. 34, pp. 2727 - 2738.

D. B. Kittelson, 1998, Engines and nanoparticles: a review. Journal of Aerosol Science, Vol. 29, pp. 575-588.

G. Lepperhoff, and M. Houben, 1993, Mechanisms of deposit formation in IC engines and heat exchangers. Society of Automotive Engineering, no. 931032.

W. J. Marner, 1990, Progress in Gas-Side Fouling of Heat-Transfer Surfaces. Applied Mechanics Reviews, Vol. 43, pp. 35-66.

A. Messerer, R. Niessner, and U.Poschl, 2003, Thermophoretic deposition of soot aerosol particles under experimental conditions relevant for modern diesel engine exhaust gas systems. Journal of Aerosol Science, Vol. 34, pp.1009-1021.

H. M. Müller-Steinhagen, and J. Middis, 1989, Particle Fouling in Plate Heat Exchanger. Heat Transfer Engineering, Vol. 10(4), pp. 30-36.

K. Nagendra, D. K. Tafti and A. K.Viswanathan, 2011, Modeling of soot deposition in wavy-fin exhaust gas

recirculator coolers. Heat and Mass Transfer, Vol. 54, pp. 1671-1681.

S. Park, K. Choi, H. Kim, and K. Lee, 2010, Influence of PM fouling on effectiveness of heat exchanges in a diesel engine with fin-type EGR coolers of different sizes. Heat and Mass Transfer, Vol. 46, pp.1221-1227.

C. Paz, E. Suárez, A. Eirís, and C. Castaño (2009). Experimental set up for the determination of fouling behaviour in diesel engine exhaust gas recirculation systems. 10th Conference on Energy for a Clean Environment, Lisbon.

C. Paz, E. Suárez, A. Eirís, and J. Porteiro, 2012, Experimental evaluation of the critical local wall shear stress around cylindrical probes fouled by diesel exhaust gases. Experimental Thermal and Fluid Science, Vol. 38, pp. 85-93.

C. Paz, E. Suárez, A. Eirís, and J. Porteiro, 2013, Development of a predictive CFD fouling model for diesel engine exhaust gas systems. Heat Transfer Engineering, Vol. 34 Issue 8-9, pp. 674-682.

C. Sluder, J. Storey, M. Lance, and T. Barone, 2013, Removal of EGR Cooler Deposit Material by Flow-Induced Shear. Society of Automotive Engineering, no. 01-1292.

R. Stauch, F. Brotz and J. Supper (2011). CFD simulation of the fouling process in EGR coolers. Vehicle Thermal Management Systems Conference, Gaydon,

A. Stolz, K. Fleischer, W. Knecht, J. Nies, and R. Strahle, 2001, Development of EGR coolers for truck and passenger car aplication. Society of Automotive Engineers, no. 2001-01-1748.

E. Suárez, C. Paz, J. Porteiro, and A. Eirís (2010). Simulation of the fouling layer evolution in heat transfer surfaces. V European Conference on Computational Fluid Dynamics, Lisbon.

H. Teng, and G. Regner, 2009, Characteristics of soot deposits in EGR coolers. Society of Automotive Engineering, no. 01-2671.

B. Thonon, S. Grandgeorg, and C. Jallut, 1999, Effect of Geometry and Flow Conditions on Particulate Fouling in Plate Heat Exchangers. Heat Transfer Engineering, Vol. 20, n°3.

M. Zheng, G. T. Reader, and J. G. Hawley, 2004, Diesel engine exhaust gas recirculation -a review on advanced and novel concepts. Energy Conversion and Management, Vol. 45, pp. 883-900.